

This article appeared in a journal published by Elsevier. The attached copy is furnished to the author for internal non-commercial research and education use, including for instruction at the authors institution and sharing with colleagues.

Other uses, including reproduction and distribution, or selling or licensing copies, or posting to personal, institutional or third party websites are prohibited.

In most cases authors are permitted to post their version of the article (e.g. in Word or Tex form) to their personal website or institutional repository. Authors requiring further information regarding Elsevier's archiving and manuscript policies are encouraged to visit:

<http://www.elsevier.com/copyright>



## Protection of NiO nanoparticles against leaching in acid medium by grafting of polyacrylic acid

Alejandro López-Ortiz, Virginia H. Collins-Martínez, Claudia A. Hernández-Escobar, Sergio G. Flores-Gallardo, E. Armando Zaragoza-Contreras<sup>\*</sup>

*Centro de Investigación en Materiales Avanzados, S.C., Miguel de Cervantes No. 120, Complejo Industrial Chihuahua, C.P. 31109 Chihuahua, Chih., Mexico*

Received 26 October 2006; received in revised form 22 November 2007; accepted 27 November 2007

### Abstract

Grafting polyacrylic acid onto the surface of nickel oxide nanoparticles was performed in order to impart to this metal oxide protection against leaching in acid solution (sulfuric acid 0.5 M). Infrared spectroscopy showed the chemical changes implicated in the different stages of the surface treatment. Open circuit potential as a function of time showed to be an excellent technique for characterizing the leaching resistance of the modified nanoparticles. This resistance was attributed to the formation of a layer of polyacrylic acid grafted and physically deposited onto the surface of the nanoparticles, which prevented the direct contact of the acid solution with the nanoparticles avoiding, consequently, leaching.

© 2007 Elsevier B.V. All rights reserved.

**Keywords:** Open circuit potential; Nickel oxide; Metal oxide protection; Nanocomposite

### 1. Introduction

One of the most commonly used metal oxides for a wide range of applications is nickel oxide (NiO). It has received considerable attention in recent years due to its catalytic, optical, electronic and magnetic properties [1–3]. Because of the volume, quantum size, surface and macroscopic quantum tunnel effects, nanocrystalline NiO is expected to possess better properties than those of micrometer-sized NiO particles [4–7]. Carnes and Klabunde [1] reported that NiO nanoparticles are much more effective catalysts than commercial NiO powder for catalytic reduction reactions. NiO behaves as a p-type semiconductor especially if thermally treated at moderate temperatures ranged between 300 and 700 °C [8,9]. Non-stoichiometric NiO solid contains some trivalent nickel ions, which are considered as lattice defects contributing to its extrinsic electric conductivity.

The development of micro-devices, such as batteries and its components, is one of the most promising applications of NiO nanoparticles [10]. In these and many other applications the

chemical stability against acid environments is crucial for the desired performance and long life of such devices, since these nanoparticles are highly susceptible to be leached out into the electrolyte due to the aggressiveness of the medium [11].

A strategy to mitigate the chemical attack of an acid environment on NiO is proposed in this research. This consisted in modifying the NiO chemical properties through integrating into an inorganic nanoparticle–polymer nanocomposite. NiO nanoparticle resistance to leaching was improved by a two-step surface chemical modification: First, a methacryl organosilane compound was linked onto the nanoparticle surface, and second, by conventional free radical polymerization chains of polyacrylic acid (PAA) were grafted on the methacryl groups.

The assessment of open circuit potential (OCP) *versus* time (*t*) was performed as the main characterization technique with the aim of evaluating the dynamic response of the leaching process taking place within an aggressive environment and the chemical stability behavior of the polymeric nanocomposite, NiO nanoparticle–PAA, as a function of time. These tests also provided essential information about the leaching rate of the nanocomposite, which will help as a criterion of screening for the polymeric material to be further improved. The tests of OCP *versus t* were run in a sulfuric acid solution (0.5 M) at laboratory-room temperature. Polymeric nanocomposite materials were tested using the carbon paste electrode technique (CPE).

<sup>\*</sup> Corresponding author at: Centro de Investigación en Materiales Avanzados, S.C., Miguel de Cervantes No. 120, Complejo Industrial Chihuahua, C.P. 31109 Chihuahua, Chih., Mexico. Tel.: +52 614 439 4811.

E-mail address: [armando.zaragoza@cimav.edu.mx](mailto:armando.zaragoza@cimav.edu.mx) (E.A. Zaragoza-Contreras).

CPE was first introduced for organic polarography by Adams in 1958 [12]. Since then CPE has mainly been used for analytical purposes in organic and inorganic systems [13–15]. The CPE arrangement consisted of two components: a nanometer-size carbon and a binder. The binder can either have electrical conducting or non-conducting properties. A CPE with a non-conducting binder can be regarded as an inert electrode in the same sense as a Pt electrode. A CPE with an electro-active polymeric composite material introduced into the carbon paste is termed as a carbon paste electro-active electrode (CPEE). Due to its hydrophobic nature, the electrolyte is not expected to penetrate into the electrode, thus the electrochemical reactions take place only at the interface. Thus by mixing the material in study with carbon paste or attaching a thin film of this material onto the CPE, it is possible to study the electrochemical reactions that take place within the electrode [15].

## 2. Experimental

### 2.1. Materials

The following reagents were used during the experimentation: 10 nm nickel oxide nanoparticles (Nanostructured & Amorphous Materials, Inc.), methacryloxypropyl trimethoxysilane (Z-6030 of Dow Corning), acrylic acid (Aldrich Co.), potassium persulfate (Aldrich Co.), acetic acid (J.T. Baker), sulfuric acid (J.T. Baker), silicone oil (Aldrich Co.), carbon Vulcan XC72 (Cabot) and bi-distilled water. All reagents were used as received.

## 3. Nanocomposite preparation

### 3.1. Methacryloxypropyl trimethoxysilane linking

NiO nanoparticles were modified as follows: 0.2 mL of methacryloxypropyl trimethoxysilane  $[\text{Si}(\text{OCH}_3)_3\text{CH}_2\text{CH}_2\text{OOC}-\text{C}(\text{CH}_3)=\text{CH}_2]$  were added to 20 mL of an aqueous solution of acetic acid (pH 2); once the organosilane was completely dissolved 0.2 g of NiO nanoparticles were incorporated into the solution and let to react for 1 h; finally the mixture was introduced to an oven at 110 °C for 6 h in order to evaporate the water and to accelerate the reaction.

### 3.2. Grafting of polyacrylic acid

The NiO nanoparticle–polyacrylic acid nanocomposite was obtained as follows: The treated nanoparticles (0.2 g) of the previous step were dispersed in 90 g of an acrylic acid (AA) solution (10 g of AA/80 g of water); afterwards the system was bubbled with nitrogen for 20 min in order to displace the oxygen dissolved in the water and to avoid a long induction period; next the system was heated to 60 °C, and a solution of potassium persulfate (0.1 g of KPS/10 mL of water) was fed to the reactor to initiate the polymerization. The polymerization was left for 2 h with mechanical agitation (300 rpm).

## 4. Characterization

### 4.1. Infrared spectroscopy

Both unmodified and modified NiO nanoparticles, and NiO nanoparticle–PAA nanocomposite were characterized by

infrared spectroscopy (FTIR) using a Nicolet Magna-IR Series II spectrometer. Before characterization all samples were dried at 120 °C for 12 h. The analyses were run using the KBr pellet technique; KBr was also used as the reference material to acquire background.

### 4.2. Differential scanning calorimetry

Glass transition temperature ( $T_g$ ) of both NiO nanoparticle–PAA nanocomposite and a control of PAA (obtained under the same conditions as the nanocomposite) were determined by differential scanning calorimetry (DSC). Thermograms were run in a TA Instruments Thermal Analyst 2100 calorimeter. All samples were first heated from room temperature to 220 °C, then cooled to 40 °C to erase thermal history, and heated again to 220 °C.  $T_g$  values were taken from the second heating process. The samples were run under air atmosphere and heating speed of 10 °C min<sup>-1</sup>.

### 4.3. Preparation of the carbon past electrodes

The carbon paste electrodes (CPE) were prepared as follows: 0.3 g of carbon Vulcan XC72 and 0.3 mL of silicone oil were mixed thoroughly in a mortar to form a homogeneous paste. Afterwards a mixture of 0.1 g of the material in study and 0.1 g of the previously prepared carbon paste were introduced and carefully compacted into a polyethylene tube of 0.2 cm of inner diameter; an additional amount of carbon paste was added to let one of the ends of the tube available for testing purposes. Latter a thin wire of Pt was inserted in the middle of the tube and drew downwards to the bottom of the tube, to provide with the needed electrical conductivity for OCP measurements. The prepared electrodes were kept in a desiccator until application. This technique of preparation has been reported previously [13,15].

### 4.4. Test of open circuit potential versus time

The tests of open circuit potential *versus* time (OCP *versus*  $t$ ) were performed at laboratory-room temperature using a Solartron Electrochemical Interphase SI1287 coupled with a PC. Tests lasted for about 20 h. The glass-made electrochemical cell contained a temperature probe, the previously prepared carbon paste electro-active electrode (CPEE) as a working electrode and finally an  $\text{Hg}/\text{Hg}_2\text{SO}_4/\text{H}_2\text{SO}_4$  (SAE,  $E=0.668$  V/NHE) electrode as reference electrode. The electrolyte used in the cell was a solution of sulfuric acid 0.5 M prepared with bi-distilled water. Agitation was provided by using a magnetic stirred plate. The obtained potentials are reported against the normal hydrogen electrode (NHE).

## 5. Results and discussion

The surface chemical modification of NiO nanoparticles could be visualized as described in Fig. 1. A requested condition to achieve a successful modification with organosilanes is the presence of hydroxyl groups on the compound which is under treatment. NiO has a hydrated crystalline structure which made

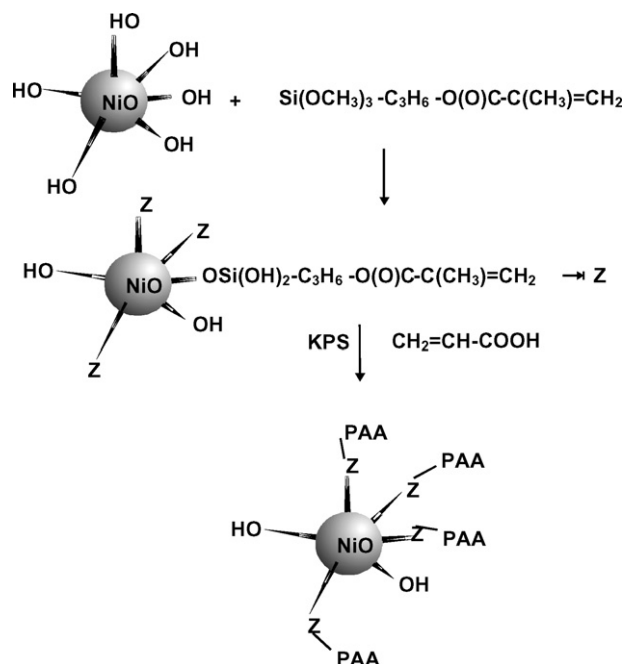


Fig. 1. Scheme of the surface modification of the NiO nanoparticles. Z represents the methacryloxypropyl trimethoxysilane groups bonded to the NiO in the first stage. PAA represents chains of polyacrylic acid grafted on the surface of the NiO nanoparticles in the second stage.

it susceptible to be modified via silanation. Once the methacryloxypropyl trimethoxysilane has been entangled, the grafting of PAA chains was performed from the double bonds  $\text{C}=\text{C}$  of the methacryl segment  $[-\text{O}(\text{O})\text{C-C}(\text{CH}_3)=\text{CH}_2]$ . It is worth mentioning that in order to corroborate methacryloxypropyl trimethoxysilane susceptibility to free radical polymerization a suspension polymerization was performed; the experiment, initiated by potassium persulfate, indicated a 95% conversion after 2 h of polymerization. Thus grafting PAA onto the organosilane is expected to occur. In addition it can be mentioned that literature shows several reports where acrylic organosilanes have been used as coupling agents between inorganic nanoparticles and organic polymers such as poly(methyl methacrylate), polystyrene and some others [16–19].

### 5.1. FTIR

The spectrum of FTIR of the NiO nanoparticles is exhibited in Fig. 2. The spectrum showed the following signals: The peaks at  $3497$  and  $1629\text{ cm}^{-1}$ , have been reported to correspond to vibrations of the bond  $\text{H-O}$  of physisorbed and chemisorbed water linked to NiO [20]; the peak at  $1346\text{ cm}^{-1}$  likely corresponds to some remnant of the precursor materials used to synthesize the NiO, as explained in literature [21,22]. The vibration of the group  $\text{Ni-O}$ , as literature indicates, should appear close to  $400\text{ cm}^{-1}$  [20,23]. However, this peak is in the limit of the spectrum and, unfortunately, cannot be observed.

The FTIR spectrum of the product of the first step of modification is shown in Fig. 3, in this reaction molecules of methacryloxypropyl trimethoxysilane were bonded to the surface of NiO nanoparticles. In the spectrum appeared the fol-

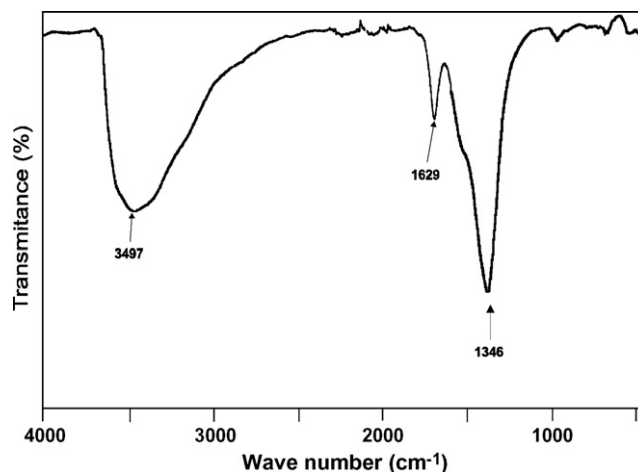


Fig. 2. FTIR spectrum of the NiO nanoparticles without treatment.

lowing signals: At  $3497\text{ cm}^{-1}$  the peak corresponding to the  $\text{H-O}$  groups in the NiO and the silane (due to acid hydrolysis); at  $2927$  and  $2960\text{ cm}^{-1}$  the peaks for the vibrations of the  $\text{C-H}$  bond of the propyl group; at  $1717\text{ cm}^{-1}$  the peak corresponding to the  $\text{C=O}$  group of the methacryl radical, the presence of this peak is important, since it indicated that the methacryloxypropyl trimethoxysilane reacted with the NiO; the peak at  $1635\text{ cm}^{-1}$  can be attributed to absorbed water as explained above for the NiO (at  $1629\text{ cm}^{-1}$ ). Fig. 4 depicts the spectrum of FTIR for the NiO nanoparticle–PAA nanocomposite, since the amount of PAA was much higher than the amount of NiO in the samples, in this figure the signals corresponded mainly to PAA. The signals in this figure were assigned as follows: at  $1695\text{ cm}^{-1}$  the peak for the  $\text{C=O}$  group of the carboxylic acid; at  $2937$  and  $1451\text{ cm}^{-1}$  the peaks for the  $\text{C-H}$  bonds of the  $\text{CH}_2$  groups; at  $1412\text{ cm}^{-1}$  the peak for the  $\text{C-OH}$  group and at  $795\text{ cm}^{-1}$  the peak for the  $\text{C-H}$  bonds of the polymeric chain.

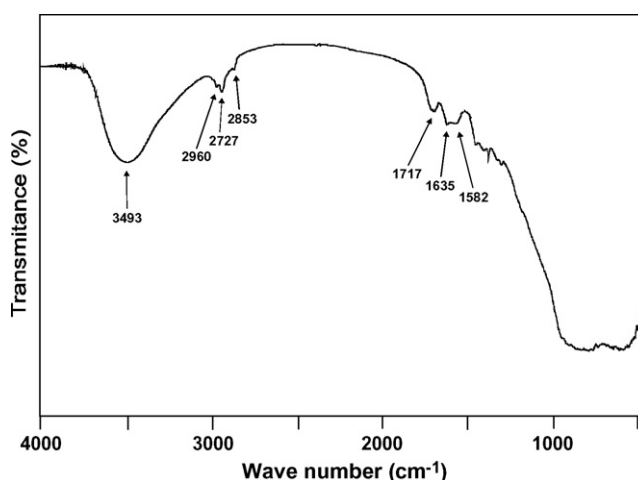


Fig. 3. FTIR spectrum of the product of reaction of the NiO nanoparticles and the methacryloxypropyl trimethoxysilane.

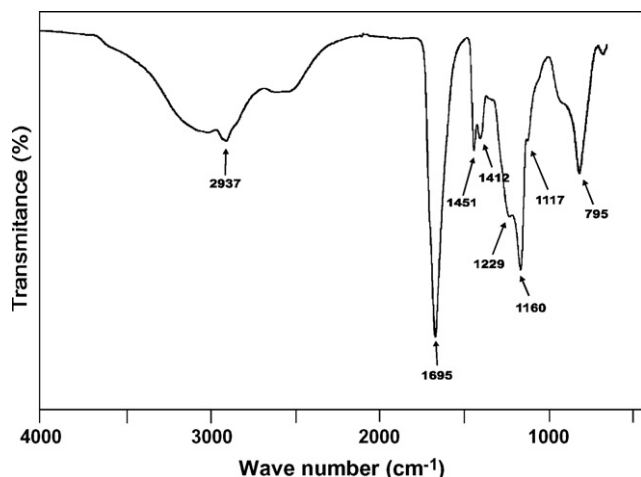


Fig. 4. FTIR spectrum of the NiO nanoparticle–methacryloxypropyl trimethoxysilane–PAA nanocomposite.

### 5.2. DSC

An increment of 4 °C on the glass transition temperature ( $T_g$ ) of the NiO nanoparticle–PAA nanocomposite with respect to the control of PAA was observed, Fig. 5. This sort of effect in the  $T_g$  has been reported to obey to motion restrictions of the polymer chains at the interface nanoparticle/matrix [24,25]. When the polymer chains have strong interfacial affinity with the filler surface, a region of polymer chains toughly tighten is formed. Such region, referred as bounded polymer layer [26] and more recently proposed as interaction zone [19], has been speculated to be some few to some tens of nanometers. At this zone or region the polymer chains exhibit a different thermal behavior with respect to the bulk, since the strong packing hindered chain mobility, which occurs under standard conditions at the  $T_g$ . Thus more energy was required to allow the first thermal transitions, shifting  $T_g$  to higher temperatures.

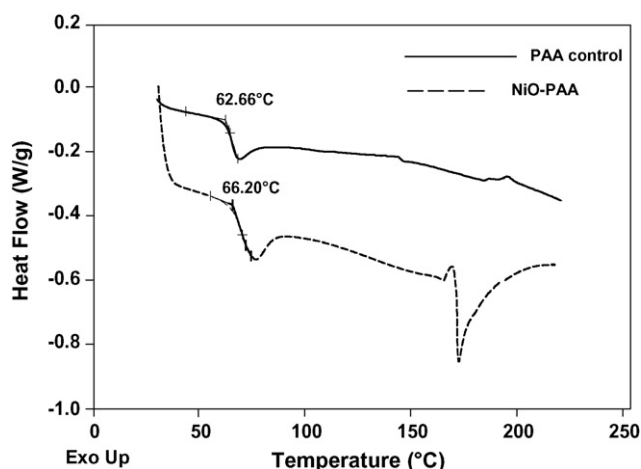


Fig. 5. DSC thermograms. The solid line corresponds to the sample of PAA control, the broken line corresponds to the NiO nanoparticle–methacryloxypropyl trimethoxysilane–PAA nanocomposite.

### 5.3. Test of OCP versus $t$

The theoretical response that can be expected in a test of OCP versus  $t$  of an electrode composed by a mixture of nickel oxide and carbon Vulcan (support), when it is exposed to a solution of sulfuric acid 0.5 M, can be related to the concentration of metal oxide present in the electrode. When the potential of the electrode increase to a stable value, the final potential reached represents the concentration of the metal oxide being in equilibrium with the electrolyte solution without any important chemical reaction taking place. On the other hand, a decrease in OCP response can be related to a reduction in concentration of the metal oxide present in the electrode and therefore, the metal oxide is being sulfated and, ultimately, leached. This behavior is consistent with a loss of metal oxide in the electrode causing a drop in the observed potential during the test. In the case that OCP remained unchanged this indicates that no material has been lost during the exposure of the electrode to the acid solution; consequently the concentration of the metal oxide remained constant within the electrode. This behavior indicates that the material was chemically stable in the system.

The possible responses of the test of OCP versus  $t$  of a metal oxide being exposed to a solution of sulfuric acid 0.5 M are shown in Fig. 6. In this figure the solid line represents the behavior of a metal oxide which is completely stable to the acid medium, since there is no change in potential at steady state conditions. The leaching rate of the metal oxide within the electrode can be assumed to present a value of zero ( $dE/dt = 0$ ). Hence the concentration of the metal oxide within the electrode can be assumed to remain without change and no leaching took place on the metal oxide. Otherwise when leaching takes place on the metal oxide, the behavior can be represented by the dashed line as shown in Fig. 6. Here the slope of the OCP versus  $t$  curve represents the leaching kinetic rate of the metal oxide ( $dE/dt \neq 0$ ), where metal oxide concentration within the electrode decreased progressively while the OCP also decreased.

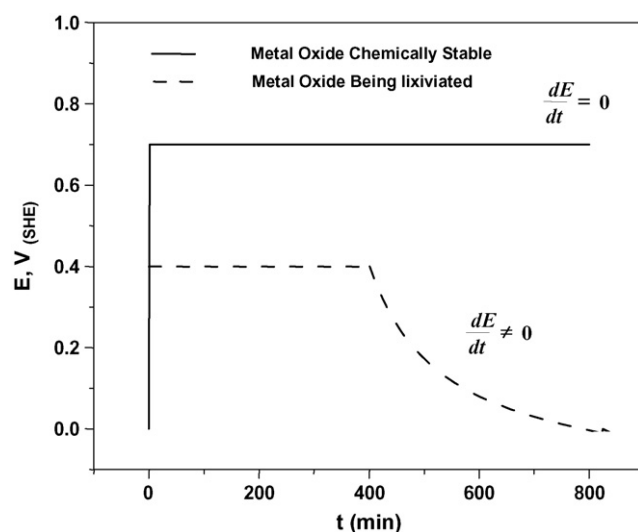


Fig. 6. Theoretical OCP vs.  $t$  responses of nickel oxide exposed to the solution of sulfuric acid 0.5 M.



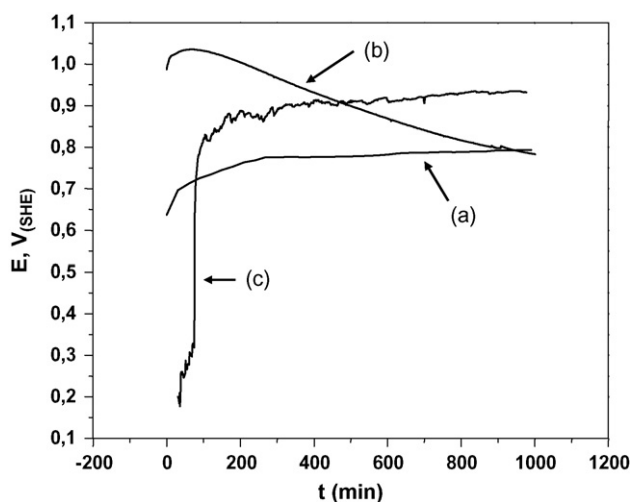


Fig. 7. OCP vs.  $t$  plots in sulfuric acid 0.5 M for: (a) electrode of carbon Vulcan XC72, (b) electrode of nickel oxide without surface treatment, and (c) electrode of NiO–PAA nanocomposite.

The first test was aimed to determine the effect of the acid medium on a control electrode of carbon Vulcan alone. Fig. 7(a) shows the response of the electrode of carbon Vulcan after 20 h of exposure to the sulfuric acid 0.5 M. As can be seen, carbon Vulcan presented an open circuit potential near to 0.78 V; according to this response it can be presumed that the initial increase of open circuit potential was due to the ionic transport of  $\text{SO}_4^{2-}$  ions to the interior of the carbon electrode. Therefore, the final potential after 20 h indicated that the electrode has been saturated with electrolyte solution and no important ionic transport occurred.

Fig. 7(b) presents the OCP dynamic response of the unprotected NiO nanoparticles in acid medium. As observed, the response of the OCP versus  $t$  curve of the NiO resulted in an initial increment of the OCP to a value of about 0.97 V after 4 min of started the test; this potential decreased monotonically with time and after 20 h a stable OCP lecture of 0.806 V was registered, this value was comparable to the value for carbon Vulcan (0.78 V). This behavior suggested that the only presence of the acid in contact with the NiO conducted to the progressive formation of nickel sulfate (Eq. (1)) and its corresponding dissolution into the electrolyte. Therefore, the fast kinetics of leaching made clear the extreme vulnerability of NiO in the presence of an acid medium.

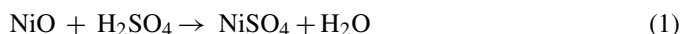


Fig. 7(c) shows the curve of OCP versus  $t$  for the protected NiO nanoparticles. In this plot it can be observed that the potential remained unchanged once it reached a steady value of about 0.87 V. This behavior evidenced the resistance of the nanocomposite towards leaching after 20 h of exposure to the aggressive acid medium. It is believed that the formation of a continuous

layer of PAA both grafted and physically deposited on the surface of the NiO nanoparticles was the cause for the resistance. Apparently the layer played the role of either chemical or permeable barrier against the acid solution preventing the direct contact with the nanoparticle. Consequently, the nanoparticles were isolated from the aggressive medium and the leaching was restricted.

## 6. Conclusion

It was possible to impart leaching resistance to nickel oxide nanoparticles by a superficial grafting of polyacrylic acid. Such resistance was attributed to the formation of a layer of polyacrylic acid, chemically and physically bonded, which restricted the direct contact of the acid solution and the nanoparticles. As a consequence the reaction of the nickel oxide and the sulfate anions to form nickel sulfate, was avoided; that is, leaching was inhibited. Complementarily it is worth mentioning that open circuit potential versus time technique was an excellent method to follow in real time the behavior of the different kinds of samples of nickel oxide exposed to the acid medium.

## References

- [1] C.L. Carnes, K.J. Klabunde, J. Mol. Catal. A, Chem. 194 (2003) 227.
- [2] V. Biju, M.A. Khadar, Mater. Sci. Eng.: A 304–306 (2001) 814.
- [3] Y. Ichihayagi, N. Wakabayashi, J. Yamazaki, S. Yamada, Y. Kimishima, E. Komatsu, H. Tajima, Physica B 329–333 (2003) 862.
- [4] L. Wu, Y. Wu, H. Wei, Y. Shi, C. Hu, Mater. Lett. 58 (2004) 2700.
- [5] X. Yi, D. Zhong, Mater. Lett. 58 (2004) 276–280.
- [6] D.L. Tao, F. Wei, Mater. Lett. 58 (2004) 3226.
- [7] V. Biju, M.A. Khadar, Spectrochim. Acta Part A 59 (2003) 121.
- [8] A. Bielanski, R. Dzeinbaj, J. Slozynski, Bull. Acad. Pol. Sci. 14 (1966) 569.
- [9] M.E. Dry, F. Stone, Discuss. Faraday Soc. 58 (1959) 192.
- [10] K.-F. Chiu, C.Y. Chang, C.M. Lin, J. Electrochem. Soc. 152 (6) (2005) A1188–A1192.
- [11] W. Mulak, B. Miazga, A. Szymczycha, Int. J. Miner. Process. 77 (4) (2005) 231–235.
- [12] R.N. Adams, Anal. Chem. 30 (1958) 1576.
- [13] E. Ahlberg, J. Asbjörnsson, Hydrometallurgy 34 (1993) 171–185.
- [14] I. Cisneros, M. Oropeza, I. Gonzalez, Hydrometallurgy 53 (1999) 133–144.
- [15] M. Rice, G. Zbigniew, R. Adams, J. Electroanal. Chem. 143 (1983) 89–102.
- [16] S. Zhou, L. Wu, J. Sun, W. Shen, Prog. Org. Coating 45 (2002) 33–42.
- [17] B. Erdem, E.D. Sudol, V.L. Dimonie, M.S. El-Aasser, J. Polym. Sci. Part A: Polym. Chem. 38 (2000) 4419–4430.
- [18] E. Bourgeat-Lami, Ph. Espiard, A. Guyot, Polymer 23 (1995) 4339–4385.
- [19] B.J. Ash, D.F. Rogers, C.J. Wiegand, L.S. Schadler, R.W. Siegel, B.C. Benicewicz, Polym. Compos. 23 (6) (2002) 1014–1025.
- [20] P.S. Patil, L.D. Kadam, Appl. Surf. Sci. 199 (2002) 211–221.
- [21] L. Wu, Y. Wu, H. Wei, Y. Shi, C. Hu, Mater. Lett. 58 (2004) 2700–2703.
- [22] W. Xing, F. Li, Z.-F. Yan, G.Q. Lua, J. Power Sources 134 (2004) 324–330.
- [23] X.-M. Liu, X.-G. Zhang, S.-Y. Fu, Mater. Res. Bull. 41 (2006) 620–627.
- [24] P.A.O. Muisener, L. Clayton, J. D'Angelo, J.P. Harmona, J. Mater. Res. 17 (10) (2002) 2507–2513.
- [25] X. Qu, T. Guan, G. Liu, Q. She, L. Zhang, J. Appl. Polym. Sci. 97 (2005) 348–357.
- [26] P. Cousin, P. Smith, J. Polym. Sci. 32 (1994) 459.